J Incl Phenom Macrocycl Chem (2017) 89:157–166
DOI 10.1007/s10847-017-0742-4

ORIGINAL ARTICLE

New DTPA-derived bis-naphthalenophanes: fluorescence, protonation, and complexation with aromatic amines

Blanca A. Durazo-Bustamante[1] · Reina Vianey Quevedo-Robles[1] · Motomichi Inoue[1] · Jose-Zeferino Ramirez[1] · Hisila Santacruz[1] · Rosa Elena Navarro[1] · Lorena Machi[1]

Received: 21 March 2017 / Accepted: 26 July 2017 / Published online: 1 August 2017

Abstract Two fluorescent, water-soluble bis-naphthalenophane isomers with six carboxylate arms, abbreviated as (bis-dtpa14nap)H_6 and (bis-dtpa15nap)H_6, were synthesized, which consist of two 1,4- or 1,5-substituted naphthalene rings interlinked by two diethylenetriaminepentaacetic (DTPA) chains through amide-linkages. Both DTPA-based macrocycles exhibit intense excimer and monomer emission bands, which sensitively respond to pH in three protonation steps; more sensitive is the 1,4-naphthyl isomer. The full pH-emission profiles have confirmed that the monoprotonated anion (bis-dtpanap)H_5^- is the major protonation species at the physiological pH. Fluorometric titrations at pH 7.2 have proven that the 1,4-naphthalenophane anion forms 1:1-complexes with cationic phenethylamine (formation constant, 5700 M^{-1}) and histamine (3000 M^{-1}), excluding tryptamine cation, whereas the 1,5-isomer does not react with any of the three amines. The primary binding forces are electrostatic interactions between the $CH_2CO_2^-$ arms of 1,4-naphthalenophane and the $CH_2CH_2NH_3^+$ chain of an aromatic amine. The resulting ion-pair is stabilized by encapsulation of the guest molecule in 1,4-napthalenophane cavity, while the 1,5-isomer cannot encapsulate. NMR studies have demonstrated that 1,4-napthalenophane has a higher freedom in reorientation of naphthalene rings. Such geometrical properties controlled by selection of naphthalene units are the feature of the new naphthalenophanes, and are responsible for the pH–emission profiles and the complexation.

Keywords Fluorescent chemosensors · Protonation · Inclusion complexes · Macrocycles · Aromatic amines

Introduction

Fluorescent cyclophanes, consisting of fluorophore units linked together through suitable bridging chains or spacer groups, have been proven to be a good choice for molecular recognition and ion-sensing [1–16]. Especially, water-soluble fluorescent cyclophanes attract a great deal of interest because of their potential application as sensors in biological media. In the molecular design of fluorescent cyclophanes, the cavity size, as well as the fluorogenic properties exhibited by these systems, can be tuned by varying the fluorophore moieties, the bridging units or the spacer groups. The aromatic moieties confer to cyclophanes a hydrophobic cavity capable of encapsulating specific guests, but the hydrophobicity reduces the water solubility of the molecule to limit the use in physiological conditions. A series of chelating, water-soluble, fluorescent aza-cyclophanes have been synthesized by reactions between aromatic diamines and EDTA (ethylenediaminetetraacetic) or DTPA (diethylenetriaminepentaacetic) dianhydride in our research group; aromatic units linked by amino and amide chains construct a macrocyclic frame, and pendant carboxylate arms enhance water-solubility [8–12]. One of the features of this type of fluorescent macrocycles is that potential binding sites for protonation and complexation are integrated within the macrocyclic frame so that direct influences on geometrical relation between the fluorogenic groups result in sensitive and novel

Electronic supplementary material The online version of this article (doi:10.1007/s10847-017-0742-4) contains supplementary material, which is available to authorized users.

✉ Lorena Machi
lmachi@polimeros.uson.mx

[1] Departamento de Investigación en Polímeros y Materiales, Universidad de Sonora, 83000 Hermosillo, SON, Mexico

response of the emission to protonation and complexation. Compared with benzene-based macrocycles, naphthalene compounds are expected to have better-defined frameworks and higher sensing capacities related to excimer emission, and these characteristics can be controlled by selection of geometrical isomers with different substitution positions. In this work, we have synthesized two new naphthalenophane isomers, **1** and **2** in Scheme 1, by the reactions of DTPA dianhydride with 1,4- and 1,5-diaminonaphthalene, respectively: **1** is 2,12,25,35-tetraoxo-4,7,10,27,30,33-hexakis(carboxymethyl)-1,4,7,10,13,24,27,30,33,36-decaaza-[13.13](1,4)naphthalenophane, abbreviated as (bis-dtpa14nap)H_6 with acidic protons, and **2** is 2,12,25,35-tetraoxo-4,7,10,27,30,33-hexakis(carboxymethyl)-1,4,7,10,13,24,27,30,33,36-decaaza-[13.13](1,5)naphthalenophane, abbreviated as (bis-dtpa15nap)H_6. Either naphthalenophane composed of two naphthyl groups is soluble in water, and exhibits intense excimer and monomer emission bands, which respond sensitively to pH. The correlations of the excimer emission with protonation and a consequent conformational change have been studied by ^{1}H NMR, in connection with the rotational freedom of naphthalene rings in the two isomers. Since the conformational property is expected to control the complexation capacity towards specific substrates as well, complexation has been tested by fluorometric titrations for cationic amines composed of different types of aromatic groups with different ring sizes; they are phenethylamine, histamine and tryptamine, chosen from bioactive amines. Selective complexation has been proven for naphthalenophane **1**, which forms a 1:1-complex with phenethylamine and histamine, while the isomer **2** does not complex with any amines.

Experimental

Syntheses of (bis-dtpa14nap)H_6

A dimethylformamide (DMF) solution (60 mL) containing 0.225 g (1.42 mmol) of 1,4-diaminonaphthalene (Aldrich) was added dropwise, through a dropping funnel, to 0.530 g (1.48 mmol) of DTPA dianhydride in 300 mL of DMF with vigorous agitation over a period of 4 h. After the resulting reaction mixture was left to stand overnight, any solid formed was removed by filtration, and the filtrate was concentrated to a viscous liquid. Addition of acetone (125 mL) gave an orange solid, which was separated by filtration, washed with acetone and dried in vacuum. The crude product was dissolved in water by adding a minimum quantity of solid Li_2CO_3, and the remaining carbonate was removed by filtration.

Scheme 1 Naphthalenophanes and guest amines chosen in this study and their abbreviations

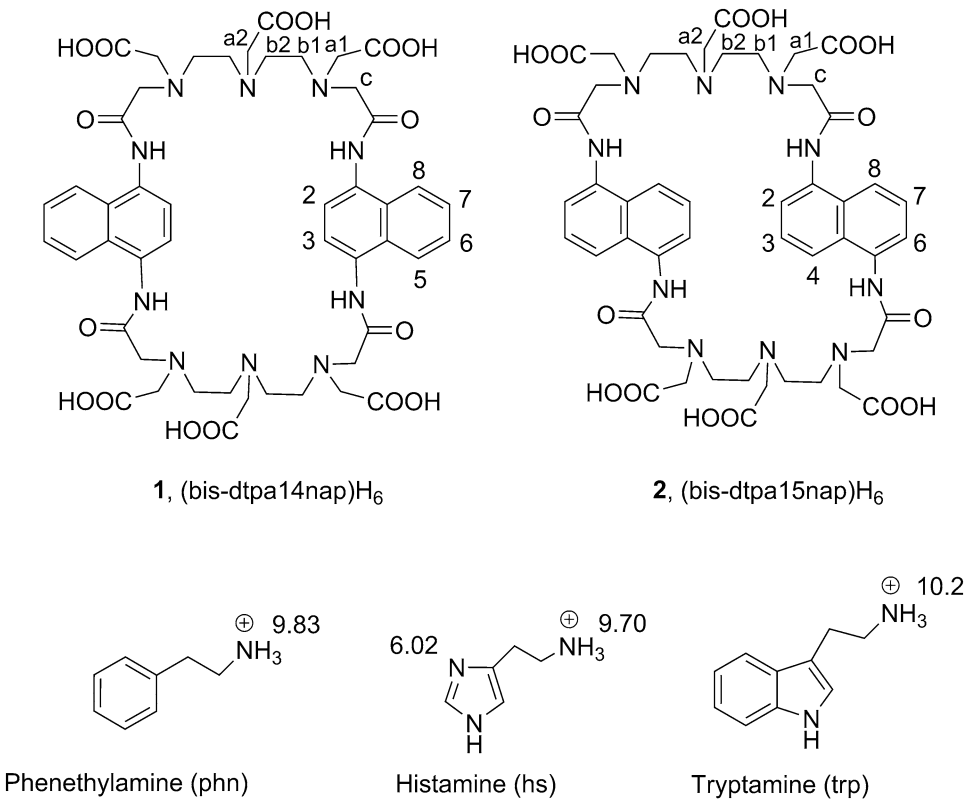

Acidification of the solution to pH 4 with dilute HCl precipitated the 2+2 reaction product. After the treatment of the solid with Li_2CO_3 and HCl was repeated, the solution was acidified to pH 2 with 0.1 M HCl, and the pure compound was obtained in the acid form. The product was washed thoroughly with water and dried in vacuum. Yield (0.041 g, 5.6%). M.p. 253–254 °C. Anal. Calcd. for $C_{48}H_{58}N_{10}O_{16}\cdot 6H_2O$: C, 50.61; H, 6.19; N, 12.30. Found: C, 50.47; H, 6.24; N, 12.6. ^{1}H NMR (D_2O, 400 MHz, pD = 11.0) δ = 3.01 (br, 8H, H_{b1} in Scheme 1), 3.04 (br, 8H, H_{b2}), 3.34 (s, 4H, H_{a2}), 3.44 (s, 8H, H_{a1}), 3.56 (s, 8H, H_c), 7.11 (dd, J = 6.2, 3.1 Hz, 4H, H_6), 7.39 (s, 4H, H_2), 7.46 (dd, 4H, J = 6.4, 2.8 Hz, H_5). ^{13}C NMR (D_2O, 100 MHz, pD = 10.97) δ = 52.4 (C_{b1}), 52.6 (C_{b2}), 57.4 (C_{a2}), 58.7 (C_{a1}), 58.9 (C_c), 121.9 ($C_{1,4}$), 122.4 ($C_{5,8}$), 126.5 ($C_{2,3}$), 128.6 ($C_{6,7}$), 130.4 ($C_{9,10}$), 164.9 (C_{amide}), 174.7 (C_{a1}–*C*OOH), 179.4 (C_{a2}–*C*OOH). HR MS ESI m/z (%) = 1029.395 (100) $[M-H]^-$ $C_{48}H_{57}N_{10}O_{16}$ (calcd. m/z = 1029.394).

Syntheses of (bis-dtpa15nap)H_6

(Bis-dtpa15nap)H_6 was synthesized by essentially the same method as for (bis-dtpa14nap)H_6 from DTPA dianhydride (3.08 g, 8.62 mmol in 300 mL of DMF) and 1,5-diaminonaphthalene (1.4 g, 8.85 mmol in 70 mL of DMF). The crude product (a purple solid) was dissolved in water with a minimum quantity of solid Li_2CO_3, and any solid present was removed by filtration. Adjustment of the pH of the solution to 3.7 with dilute HCl gave the pure product. For conversion into the pure acid, the solid was dissolved again with Li_2CO_3, and the resulting solution, after being filtered, was acidified to pH 2 with 0.1 M HCl. The precipitate was washed thoroughly with water and dried in vacuum. Yield (0.298 g, 6.5%). M.p. 255–256 °C. Anal. Calcd. for $C_{48}H_{58}N_{10}O_{16}\cdot 5H_2O$: C, 51.42; H, 6.11; N, 12.49. Found: C, 51.70; H, 6.05; N, 12.47. ^{1}H NMR (D_2O, 400 MHz, pD = 11.06) δ = 3.00 (br, 8H, H_{b1}), 3.03 (br, 8H, H_{b2}), 3.34 (s, 4H, H_{a2}), 3.43 (s, 8H, H_{a1}), 3.53 (s, 8H, H_c), 7.28 (d, J = 8.1 Hz, 4H, $H_{2,6}$), 7.34 (t, J = 7.7 Hz, 4H, $H_{3,7}$), 7.52 (d, J = 6.9 Hz,4H, $H_{4,8}$). ^{13}C NMR (D_2O, 100 MHz, pD = 8.7) δ = 49.9 (C_{b1}), 53.4 (C_{b2}), 53.7 (C_{a2}), 57.7 (C_{a1}), 58.0 (C_c), 121.4 ($C_{4,8}$), 123.1 ($C_{3,7}$), 125.5 ($C_{2,6}$), 128.2 ($C_{1,5}$), 131.0 ($C_{9,10}$), 170.5 (C_{amide}), 173.7 (C_{a1}–*C*OOH), 178.7 (C_{a2}–*C*OOH). HR MS ESI m/z (%) = 1029.400 (100) $[M-H]^-$ $C_{48}H_{57}N_{10}O_{16}$ (Calcd. m/z = 1029.394).

The mass spectra were obtained for NH_3–methanol solutions at the University of Arizona Mass Spectroscopy Facility (Tucson, AZ, USA). The elemental analyses were performed by ALS Environmental (Tucson, AZ, USA).

Spectroscopic measurements and protonation

Luminescence spectra were recorded on a Perkin-Elmer LS-50B luminescence spectrometer. Sample compounds were dissolved in 0.01 M NaCl solution by adding just necessary amount of solid Na_2CO_3, and the pH was adjusted with 0.01 M HCl and 0.01 M NaOH. For experiments of pH dependence, sample solutions were prepared from two stock solutions at the lowest and highest pH in such a way that the ionic strength as well as the sample concentration was kept identical. The ^{1}H NMR spectra were obtained with a Brucker AVANCE 400 spectrometer for H_2O-d_2 solutions at a probe temperature of approximately 23 °C. Sample solutions were prepared for pD-variation experiments as follows. Two stock solutions were prepared by adding a minimal amount of solid Na_2CO_3 into suspension of a sample compound in D_2O containing 0.01% DSS (sodium 2,2-dimethyl-2-silapentane-5-sulfonate) as the internal reference, followed by adjusting the pD to the lowest and the highest values with dilute HCl-d and KOH-d solutions, respectively. Sample solutions were prepared by weighing out the stock solutions directly into NMR sample tubes in different ratios in such a way that the total weight of every sample solution was 0.5 g. The maintenance of a constant ionic strength requires an electrolyte concentration higher than 0.1 M in NMR titrations. Since such conditions cause difficulty in observing spectra of high quality, the ionic strength was not controlled in the present experiments. The pD value of each sample solution was determined after NMR measurements. A pH value measured was converted to the pD value on the basis of the relation $pD = pH_{meas} + 0.45$ [17].

Fluorometric titrations

The guest amines were supplied from Sigma-Aldrich (in 98–99% purity), and used as received. Fluorometric titrations were carried out at the physiological pH 7.2 in a 0.01 M MOPS (4-morpholinepropanesulfonic acid) buffer at a temperature of 25 °C. A quartz cuvette of the spectrometer was loaded with 3 mL of a 2×10^{-5} M solution of an appropriate naphthalenophane receptor, to which 0.02 mL aliquots of a 3×10^{-3} M solution of a selected guest compound were added successively with a calibrated micropipette in the range of titrant-to-titrate concentration ratio 0–25. Excitation wavelength λ_{ex} 315 nm was chosen for the 1,4-naphthyl isomer, and λ_{ex} 308 for the 1,5-naphthyl isomer in titrations with phenethylamine and histamine, so that the guest compounds had no interference with emission from the naphthalenophanes throughout the concentration range of the titrants. In the studies of tryptamine, λ_{ex} was 330 nm to minimize the interference of the guest. The emission intensity was corrected for a change in the

sample volume, and the ratiometry, which is independent of the fluorophore concentration, was employed for the determination of formation constants. Least-squares fittings of titration curves were performed on locally developed Excel® worksheets.

Results

Fluorescence and protonation

The new naphthalenophane isomers, which carry a number of amino and carboxylate groups as potential protonation sites, are expected to form a variety of ionic species depending on pH. Such a protonation scheme is expected to be correlated to the fluorescence, and the fluorogenic species are required to be identified prior to fluorometric studies of complexation with guest amines at a constant pH.

Figure 1 shows the emission spectra of (bis-dtpa14nap)H_6 in aqueous solutions at different pH values. Basic solutions exhibit an intense peak at λ = 380 nm and a shoulder at 408 nm. The former is characteristic of emission from monomeric naphthalene, and the latter is attributable to naphthalene excimer [18–25]. The intensity of the monomer band at 380 nm is weakened sharply with lowering pH. The tail of the spectrum band involves a hump at the longer

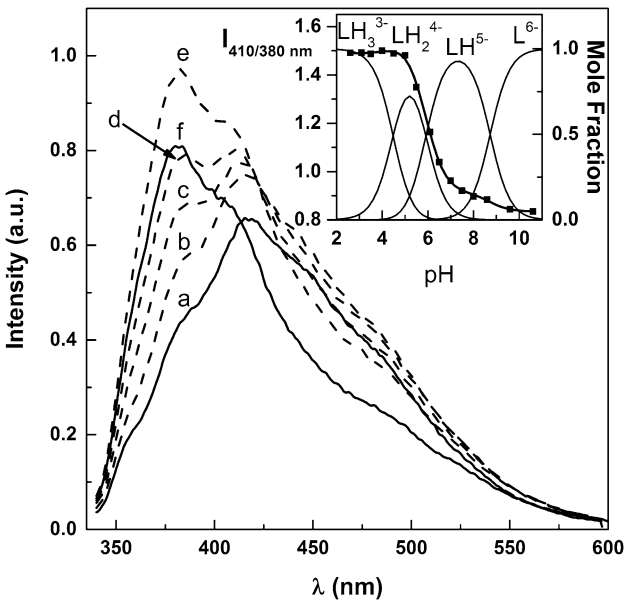

Fig. 1 Emission spectra of (bis-dtpa14nap)H_6 in 0.01 M NaCl solution at different pH values: *a* 4.5, *b* 5.5, *c* 6.0, *d* 6.5, *e* 8.6 and *f* 10.6. The excitation wavelength, λ_{exc} is 315 nm, and the concentration 2×10^{-5} M. *Inset* the intensity ratio of the 410–380 nm emissions, $I_{410}/I_{380,}$ as a function of pH, and the best fit with Eq. 1; mole fractions of protonation species (bis-dtpa14nap)$H_n^{(6-n)-}$, calculated with log K_{pn} values in Table 1

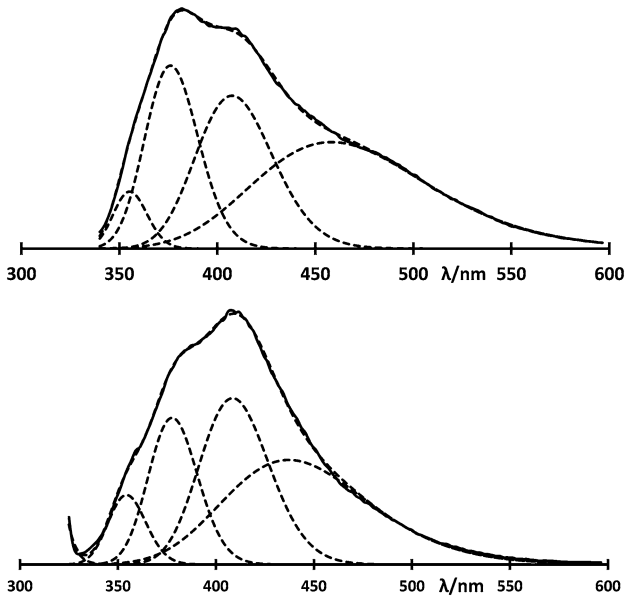

Fig. 2 Emission spectra and deconvolutions based on a Gauss distribution function of 1/λ. *Top* (bis-dtpa14nap)H_6 at pH 7.5; the component bands are centered at 458 nm (with a relative area of 1.0), 408 (0.8), 376 (0.8), and 355 (0.2). *Bottom* (bis-dtpa15nap)H_6 at pH 6.1; the components are centered at 437 nm (1.0), 409 (0.9), 378 (0.6), and 354 (0.3)

wavelength side. The spectrum deconvolution, represented in Fig. 2, demonstrates the presence of a broad band centered at 458 nm with the area comparable to that of the 408 nm band. The component band at 458 nm is also characteristic of naphthalene excimer [26]. The inset of Fig. 1 presents the ratio of intensities at 410 and 380 nm, I_{410}/I_{380}, which corresponds to the ratio of the excimer to the monomer emission, I_E/I_M. The intensity ratio increases with decreasing pH in three steps from 0.84 at pH 10.6 to the maximum 1.49 at pH 2.6. This pH dependence is related to protonation–deprotonation equilibrium as reported for fluorophores linked to donor groups [11–13, 18, 20–25, 27–31]. Among the three protonation steps, the second is the most influential to the emission.

Since protonation is responsible for the change in emission, the intensity is described by the following function of pH:

$$I(\mathrm{pH}) = [I_0 + \Sigma I_n \times \beta_{pn} \times 10^{-n\times\mathrm{pH}}]/[1 + \Sigma\beta_{pn} \times 10^{-n\times\mathrm{pH}}] \quad (1)$$

Here, I_n is the intensity inherent in species (bis-dtpa14nap)$H_n^{(6-n)-}$, and β_{pn} is the overall protonation constant which is related to the step-wise constants as $\log\beta_{pn} = \Sigma \log K_{pn}$. The logarithmic protonation constants have been determined as log $K_{p1} = 8.73$, log $K_{p2} = 5.92$ and log $K_{p3} = 4.48$ from the observed I_{410}/I_{380} versus pH curve by a non-linear least-squares curve fitting (see Table 1).

Table 1 Logarithms of the protonation constants, log K_{pn} determined by fluorescence and log K_{Dn} by ^{1}H NMR, for (bis-dtpa14nap)$^{6-}$ and (bis-dtpa15nap)$^{6-}$

L^{6-}	$\log K_{p1}$, $\log K_{D1}$*	$\log K_{p2}$	$\log K_{p3}$, $\log K_{D2}$*
1, (bis-dtpa14nap) $^{6-}$			
FL	8.73 (2)	5.92 (3)	4.48 (3)
NMR	10.55 (3)		5.94 (6)
2, (bis-dtpa15nap) $^{6-}$			
FL	8.33 (2)	6.22 (2)	3.00 (6)
NMR	10.15 (2)		5.52 (4)

*Values obtained for proton a2 in Scheme 1

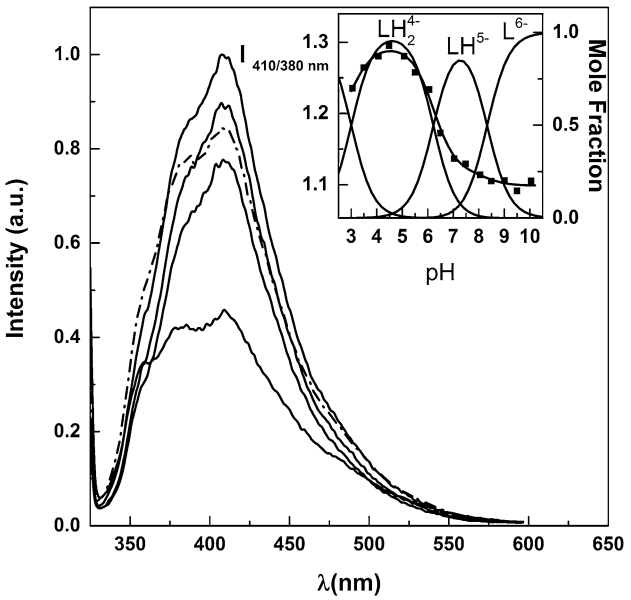

Fig. 3 Emission spectra of (bis-dtpa15nap)H_6 in 0.01 M NaCl solution at different pH values (10.0, 4.5, 8.1, 5.1, and 6.1 from the *bottom* to the *top*). The excitation wavelength, λ_{exc} is 315 nm, and the concentration 2×10^{-5} M. *Inset* the intensity ratio of the 410–380 nm emissions, $I_{410}/I_{380,}$ as a function of pH, and the best fit with Eq. 1; mole fractions of protonation species (bis-dtpa15nap)$H_n^{(6-n)-}$, calculated with log K_{pn} values in Table 1

The other bis-naphthalenophane isomer, (bis-dtpa15nap)H_6, exhibits three overlapped emission peaks at *ca*. 360, 380 and 410 nm, as exemplified in Fig. 3. The first two are attributable to emissions from monomeric naphthalene, and the third from naphthalene excimer [18, 20–25]. The spectrum extensively tails to the longer wavelength side. Spectrum deconvolution indicates the presence of another excimer band centered at *ca*. 440 nm (Fig. 2), when the widths of three component bands are assumed to be of the same extent as the corresponding band widths in (bis-dtpa14nap)H_6. The overall emission is intensified with the decrease of pH down to pH ≈ 6, and then weakened with further pH decrease. A similar trend against pH is observed for the ratio of intensities at 410 and 380 nm, I_{410}/I_{380}, as presented in the inset in Fig. 3; the ratio is 1.1 at pH 10, 1.3 (maximum) at pH 4.5, and 1.2 at pH 3. The protonation constants have been determined on the basis of Eq. 1 as shown in Table 1.

^{1}H NMR and protonation schemes

Protonation on a donor site is detected by NMR chemical shifts of protons adjacent to the donor site [32]. The δ_j of proton j is given by a function of pD:

$$\delta_j(\mathrm{pD}) = [\delta_{j0} + \Sigma_n \delta_{jn} \times \beta_{Dn} \times 10^{-n\times \mathrm{pD}}]/[1 + \Sigma_n \times \beta_{Dn} \times 10^{-n\times \mathrm{pD}}] \quad (2)$$

Here, δ_{j0} is δ_j value of the proton j in the completely deprotonated species, δ_{jn} is the δ_j values in the n-th protonation species, and β_{Dn} is the n-th overall protonation constant in D_2O. Figures 4 and 5 show the pD dependence of δ of the two isomers in the pD range 4–12.5, and the spectra in the aliphatic region are presented in Figures S1–S4 in Supplementary Materials Section; below pD 4, the solubility is too low for NMR measurements. The δ_j of every proton shows two-step pD-dependence, which gives only two log K_D values (Table 1). The K_D values of common weak acids are larger than the corresponding K_p by approximately one unit because of difference between acid dissociations in D_2O and H_2O [33], and a further difference is expected due to ionic strength

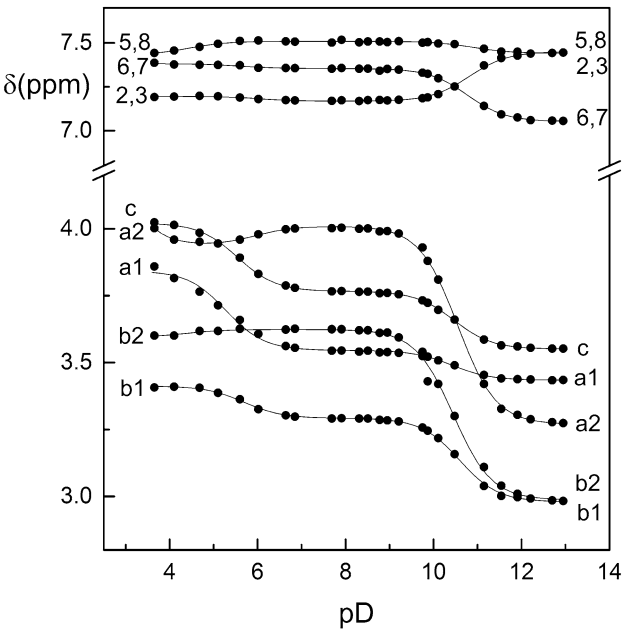

Fig. 4 pD dependence of ^{1}H NMR chemical shifts (referenced to DSS) of (bis-dtpa14nap)H_6; for labeling see Scheme 1. The *solid lines* show the best fits with Eq. 2

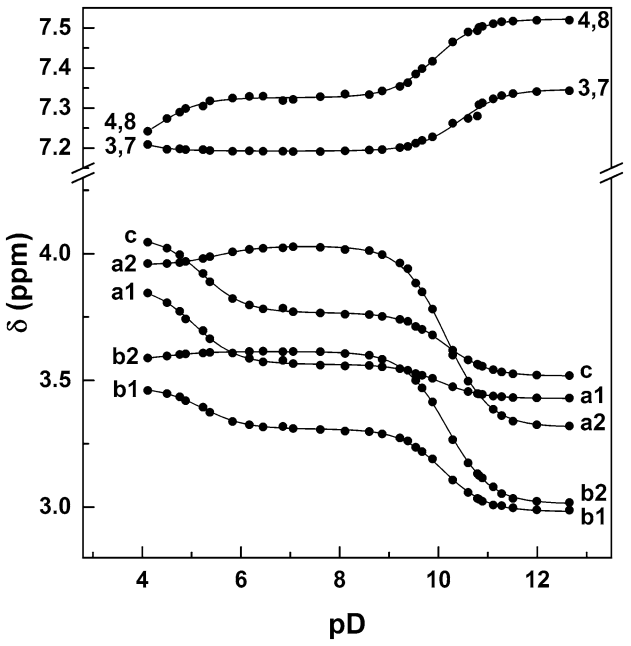

Fig. 5 pD dependence of ^{1}H NMR chemical shifts (referenced to DSS) of (bis-dtpa15nap)H_6; for labeling see Scheme 1. The *solid lines* show the best fits with Eq. 2. The signal of 2,6-proton is overlapped with the neighboring signals

[34, 35]. Therefore, the first protonation constants determined by the two methods are well correlated to each other with the difference log K_{D1}−log K_{p1} = 1.7–1.8 in both isomers. On the other hand, log K_{D2} values (5.2 and 5.9) are smaller than the corresponding log K_{p2} values (5.9 and 6.2), contrarily to the common relation, $K_{Dn} > K_{pn}$, for the same protonation process; the log K_{D2} values can be rather correlated to log K_{p3} values (4.5 and 3.0). This apparent discrepancy is ascribable to the equilibria and chemical species that the two techniques can view with their inherent observation times (~10^{-4} s of NMR and ~10^{-15} s of fluorescence spectroscopy), as explained below.

The first protonation on (bis-dtpanap)$^{6-}$ occurs mainly at the nitrogen of the central > $NCH_2CO_2^-$ group in each DTPA moiety, because the CH_2 protons in the group (protons labeled a2 and b2 in Scheme 1) show the largest change in NMR δ. The populations of acidic protons have been determined by ^{1}H NMR for DTPA-based aliphatic compounds [29, 36, 37]. By assuming the validity of the calculation method for the aromatic derivatives, proton populations in (bis-dtpa14nap)H_2^{4-} are calculated to be 0.88 on the central nitrogen in each DTPA unit, 0.04 on the central carboxylate group, and 0.04 on each of two outer amino nitrogen atoms; the corresponding values for (bis-dtpa15nap)H_2^{4-} are 0.81, 0.06, and 0.06, respectively. Basically, two acidic protons in (bis-dtpanap)H_2^{4-} are attached to nitrogen of two central > $NCH_2CO_2^-$ units. The protonation processes at the two chemically equivalent sites are expressed by the following equilibria:

$$N = N \rightleftharpoons (HN = N \rightleftharpoons N = NH) \rightleftharpoons HN = NH \quad (3)$$

Here, N=N symbolizes the two central amino nitrogen atoms linked within a macrocyclic ring in (bis-dtpanap)$^{6-}$, (HN=N ⇌ N=NH) presents micro-equilibrium between two equivalent micro-species of the first protonation product (bis-dtpanap)H^{5-}, and HN=NH shows protonation at both donor sites in (bis-dtpanap)H_2^{4-}. A change in electronic environment by protonation is localized around the donor site in the aliphatic moiety, and a time-average of the local environments is observed by NMR because the chemical equilibria are much faster than the time scale of NMR observation. As a consequence, NMR cannot distinguish between the single-protonation species (HN=N, N=NH) and the double-protonation species HN=NH; *i.e.*, NMR views the two-step protonation as if a single-step protonation occurred independently at halves the molecule, determining only log K_{D1} for (bis-dtpanap)H^{5-} and (bis-dtpanap)H_2^{4-}. By contrast, fluorescence spectroscopy with the short observation time can distinguish between (bis-dtpanap)H^{5-} and (bis-dtpanap)H_2^{4-}, because the single- and double-protonation modes lead to different molecular rigidities and consequently distinct quantum yields of emission although the micro-species in (bis-dtpanap)H^{5-} are still indistinguishable by fluorometry. Therefore, fluorometry can determine log K_{p1} and log K_{p2} associated with (bis-dtpanap)H^{5-} and (bis-dtpanap)H_2^{4-}, respectively. Thus, the two techniques give apparently different species distributions, as compared in Figs. 6 and 7. Upon further protonation, the fluorescence titration can determine log K_{p3} for the third protonation step to (bis-dtpanap)H_3^{3-}, while the NMR titration gives a single constant log K_{D2} for (bis-dtpanap)H_3^{3-} and (bis-dtpanap)H_4^{2-} because these species have the same local electronic environment around the protonation sites. Micro-protonation processes detected by NMR have been pointed out to be distinct from macro-protonation processes detected by ordinary macroscopic methods for DTPA and its derivatives in which two equivalent protonation sites are located apart [32, 36, 37]. The present study explains the distinction form different viewpoints, and suggests that full characterization of protonated species is important in the molecular design of ionic receptors. The species distributions shown in Figs. 6 and 7 conclude that the enhancement of excimer emission is a result of the protonation at the amino nitrogen of the two central > $NCH_2CO_2^-$ units in both naphthalenophanes.

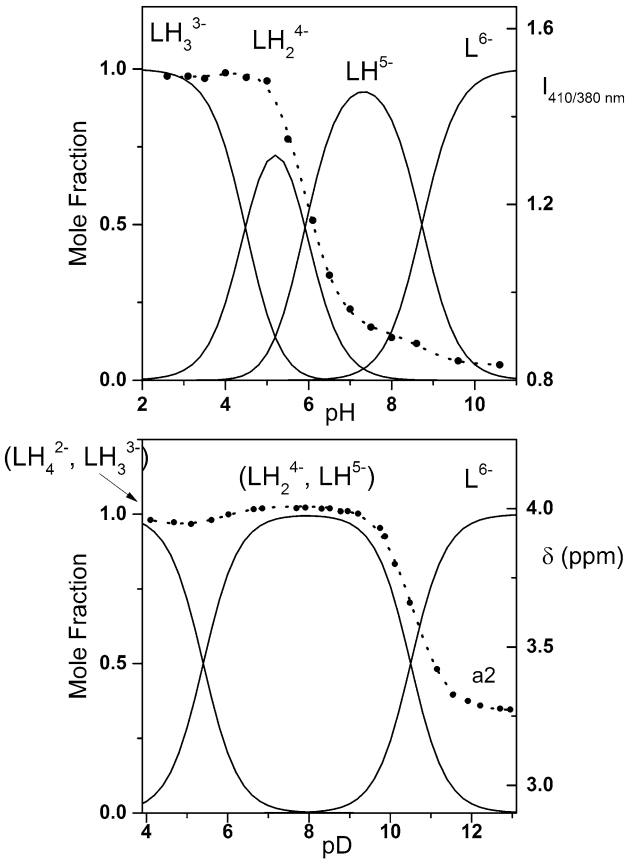

Fig. 6 Comparison of species distributions determined for (bis-dtpa14nap)$H_n^{(6-n)-}$ (denoted by $LH_n^{(6-n)-}$) by (*top*) excimer-to-monomer intensity ratio $I_{410}/I_{380\ nm}$ and (*bottom*) ^{1}H NMR shifts; the abscissa scales are displaced for the aid of comparison because of different acid dissociations in H_2O and D_2O media (for details, see the text). In each figure, the observed data are shown with the best fits (*dotted lines*) with Eq. 1 or 2; for NMR, a2 proton signal is represented

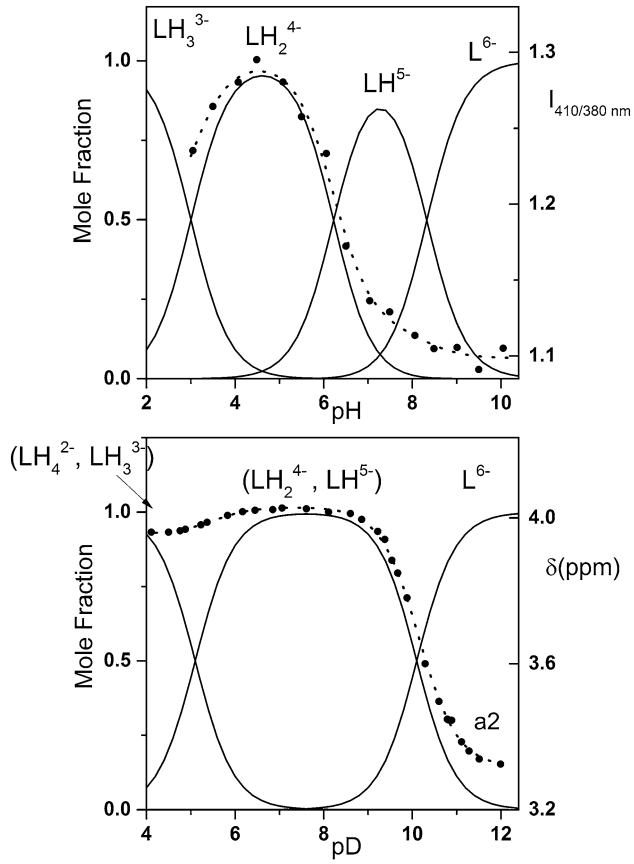

Fig. 7 Comparison of species distributions determined for (bis-dtpa15nap)$H_n^{(6-n)-}$ (denoted by $LH_n^{(6-n)-}$) by (*top*) excimer-to-monomer intensity ratio $I_{410}/I_{380\ nm}$ and (*bottom*) ^{1}H NMR shifts; the abscissa scales are displaced for the aid of comparison because of different acid dissociations in H_2O and D_2O media (for details, see the text). In each figure, the observed data are shown with the best fits (*dotted lines*) with Eq. 1 or 2; for NMR, a2 proton signal is represented

Complexation with aromatic amines

The full characterization of the protonation of the naphthalenophanes concludes that either isomer takes the mono-protonated state, (bis-dtpanap)H^{5-}, at the physiological pH 7.2. These anionic receptors (denoted by RH^{5-}) are expected to react with cationic substrates. The present study of complexation has tested three cationic amines composed of different types of aromatic groups with different ring sizes; i.e., phenethylamine, histamine and tryptamine. The pK_a values shown in Scheme 1 indicate that every amine takes the mono-cationic form (denoted by AH^+) at the physiological pH [38]. Since every reactant exits as a single species at pH 7.2 (Figs. 6, 7), the titrations determine the proper formation constants rather than the conditional.

In the titrations of the 1,4-naphthalenophane with the titrants histamine and phenethylamine, the emission responds to the guest amines as presented in Figs. 8 and 9: with increasing the guest concentration, the monomer emission strengthens with a trend of saturation whereas the intensities of the excimer emissions decrease in an asymptotic manner. The inset in each figure shows the ratio of spectrum intensities at 380 and 480 nm, $I_R = I_{480}/I_{380}$, as a function of the guest concentration, as the ratiometry compensates variation in the experimental and spectrometric conditions if any. The asymptotic decrease of the titration curves is evidence for complexation between (bis-dtpa14nap)H^{5-} anion and the aminiun cations. By contrast, tryptamine cation is inactive to the naphthalenophane anion, because the addition of tryptamine does not cause a spectral change: the shape of the emission spectrum is unchanged, and the spectrum intensity corrected for volume changes as well as for baseline due to tryptamine emission is constant throughout the titration run (Fig. 10). Thus, (bis-dtpa14nap)H^{5-} has selectivity towards histamine and phenethylamine in the complexation.

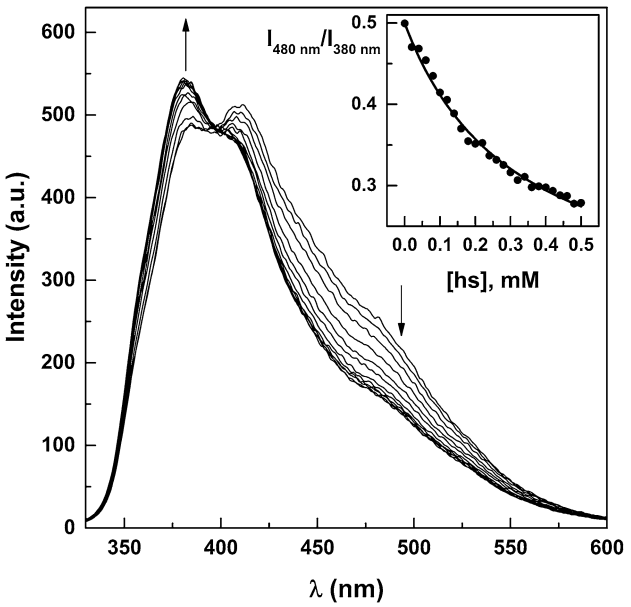

Fig. 8 Fluorometric titration of (bis-dtpa14nap)H^{5-} (2×10^{-5} M) with histamine cation (0–5×10^{-4} M): $\lambda_{ex}=315$ nm, pH = 7.2 in 0.01 M MOPS buffer, and $T=25$ °C. The *inset* plots the excimer-to-monomer intensity ratio, $I_R=I_{480nm}/I_{380\ nm}$, as a function of the total titrant concentration; the *solid line* shows the least-squares fit based on 1:1-stoichimetry with the formation constant 3000 M^{-1}

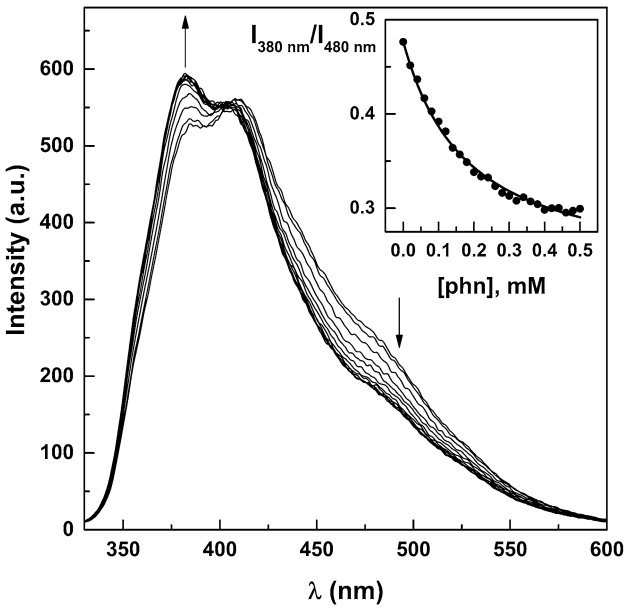

Fig. 9 Fluorometric titration of (bis-dtpa14nap)H^{5-} (2×10^{-5} M) with phenethylamine cation (0–5×10^{-4} M): $\lambda_{ex}=315$ nm, pH = 7.2 in 0.01 M MOPS buffer, and $T=25$ °C. The *inset* plots the excimer-to-monomer intensity ratio, $I_R=I_{480}/I_{380\ nm}$, as a function of the total titrant concentration; the *solid line* shows the least-squares fit based on 1:1-stoichimetry with the formation constant 5700 M^{-1}

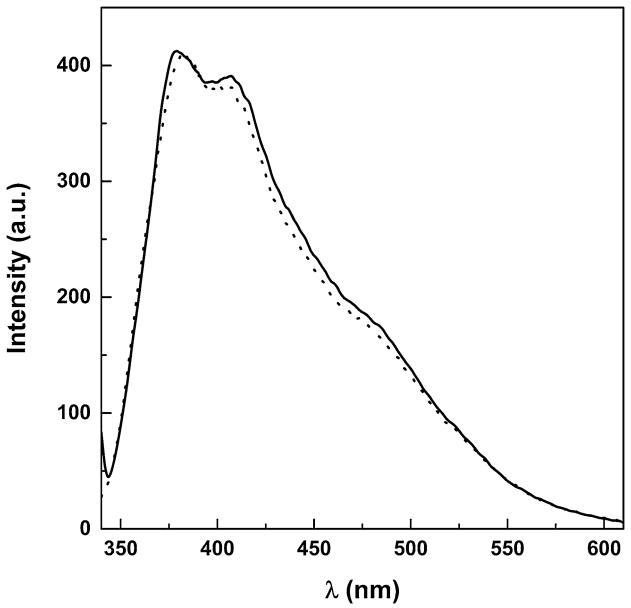

Fig. 10 Spectra observed for (bis-dtpa14nap)H^{5-} (2×10^{-5} M) in the fluorometric titration with tryptamine cation at [trp] = 0 (*solid line*) and [trp] = 5×10^{-4} M (*dotted line*); $\lambda_{ex}=330$ nm, pH = 7.2 in 0.01 M MOPS buffer, and $T=25$ °C. The spectrum at [trp] = 5×10^{-4} M is corrected for change in sample volume and for baseline due to emission from tryptamine

The asymptotic titration curves are characteristic of 1:1-complexation, which proceeds under the following equilibrium with the formation constant K_f.

$$AH^+ + RH^{5-} \rightleftharpoons AH^+RH^{5-} \quad K_f = [AR]/[A][R] \tag{4}$$

The acidic protons and charges are discarded in K_f for simplicity. Since the intensity ratio I_R is independent of the total concentration of the fluorophore, it is given by the average over the fluorophore molecules in the free and complexed sates as follows.

$$I_R = I_{RF} \times f_F + I_{RC} \times f_C \tag{5}$$

Here I_{RF} and I_{RC} are the I_R values inherent in the naphthalenophane in its free and complexed states, respectively, and f_F and f_C are the mole fractions. The curve fittings based on Eq. 5 reproduce the observed curves (Figs. 8, 9), to give the formation constant 5700 (340) M^{-1} for the phenethylamine complex and 3000 (270) M^{-1} for the histamine complex. Other stoichiometry such as A_2R did not interpret the titration curves.

In the titration of the 1,5-naphthalenophane, the shape of the emission spectrum is not changed by addition of any amine, and the peak height corrected for volume changes is unchanged throughout the titration run, in the same manner as found for the titration of the 1,4-naphthalenophane with tryptamine. Thus, none of the cationic amines forms

a complex with the 1,5-naphthalenophne, in contrast to the complexation of the 1,4-isomer.

In summary, (bis-dtpa14nap)H^{5-} recognizes cationic phenethylamine and histamine, excluding tryptamine cation, at the physiological pH. By contrast, (bis-dtpa15nap)H^{5-} cannot recognize any amine cations tested.

Discussion

The excimer-to-monomer intensity ratio (I_E/I_M) responds sensitively to pH in both bis-naphthalenophanes. The most pronounced response occurs accompanying the equilibrium between (bis-dtpanap)$^{6-}$ and (bis-dtpanap)H_2^{4-}; the protonation at the central $>NCH_2CO_2^-$ nitrogen is supposed to make the naphthyl groups oriented more favorably for the excimer formation. The ratio I_E/I_M is increased by 1.8 times in the 1,4-naphthyl isomer, but only by 1.2 times in the 1,5-naphthyl isomer. This distinction between the on–off intensity–pH profiles is supposed to be related to the rotational freedom of the naphthyl groups within the macrocyclic frameworks; the naphthyl rings bound at 1 and 4 positions can rotate about the axis through the substituted positions, whereas the 1,5-substituted groups have little freedom in their reorientation. This distinction in the freedom of reorientation can be confirmed by the pH-variable ^{1}H NMR (Figs. 4, 5). In the NMR of the 1,4-isomer, the signal of aromatic proton 2 shifts up-field with a change in δ (Δδ) of −0.3, whereas proton 6 undergoes down-field shift by Δδ = +0.3; these large shifts with the opposite signs of Δδ suggest a large change in the relative orientation of naphthyl groups, because the naphthyl protons are under the influence of strong local magnetic field induced by the ring current while the electronic state of the aromatic groups is little affected by protonation at the aliphatic amino nitrogen. In the 1,5-isomer, both protons 3 and 4 shift up-field with smaller Δδ of −0.15 and −0.19, respectively, suggesting the smaller degree of naphthyl reorientation upon protonation. These observations of NMR conclude that the substitution positions of the fluorophore control the pH-sensing capacity with the distinct on–off profiles in the naphthalene isomers.

The strong geometrical restriction, confirmed by pH-variable fluorometry and NMR, is expected to control the complexation capability as well. In fact, the fluorometric titrations have proven that (bis-dtpa14nap)H^{5-} forms complexes with cationic phenethylamine (formation constant, 5700 M^{-1}) and cationic histamine (3000 M^{-1}), whereas (bis-dtpa15nap)H^{5-} cannot react with any cationic amines tested. The primary binding forces of the (bis-dtpa14nap)H^{5-} complexes in aqueous media are electrostatic interaction between the pending $CH_2CO_2^-$ arms of the macrocycle and the lateral $CH_2CH_2NH_3^+$ group of the amine. The resulting ion-pair is stabilized by encapsulation of the guest cation in the naphthalenophane cavity through the π–π and/or hydrophobic interactions. In the process of the encapsulation by the 1,4-naphthalenophane, the naphthalene rings can reorient to adapt the macrocyclic conformation for complexation. On the other hand, the 1,5-isomer has little freedom in reorientation of naphthalene ring so that the macrocyclic cavity cannot encapsulate a guest molecules. The strong geometrical restriction due to naphthyl groups leads to the difference between the complexation capacities of the two isomers. This feature is a result of selecting naphthyl constituents with different substitution positions in the molecular design of the receptors.

Acknowledgements This work was supported in part by the Consejo Nacional de Ciencia y Tecnología de México (CONACYT, Project No. 79272, and RTQS 271884). The NMR spectrometer is operated under the support of the Secretaría de Educación Publica, México (SES-SEP, Program No. P/PIFI 2014–2015). B.A. Durazo-Bustamante is indebted to CONACYT for graduate scholarship.

References

1. Inouye, M., Fujimoto, K., Furusyo, M., Nakazumi, H.: Molecular recognition abilities of a new class of water-soluble cyclophanes capable of encompassing a neutral cavity. J. Am. Chem. Soc. **121**(7), 1452–1458 (1999). doi:10.1021/ja9725256
2. Yousuf, M., Ahmed, N., Shirinfar, B., Miriyala, V.M., Youn, I.S., Kim, K.S.: Precise tuning of cationic cyclophanes toward highly selective fluorogenic recognition of specific biophosphate anions. Org. Lett. **16**(8), 2150–2153 (2014). doi:10.1021/ol500613y
3. Qin, D.-B., Xu, F.-B., Wan, X.-J., Zhao, Y.-J., Zhang, Z.-Z.: Effectively selective fluorescent chemosensor for terephthalate. Tetrahedron Lett. **47**(32), 5641–5643 (2006). doi:10.1016/j.tetlet.2006.06.030
4. Kim, S.K., Singh, N.J., Kwon, J., Hwang, I.-C., Park, S.J., Kim, K.S., Yoon, J.: Fluorescent imidazolium receptors for the recognition of pyrophosphate. Tetrahedron. **62**(25), 6065–6072 (2006). doi:10.1016/j.tet.2006.03.107
5. Neelakandan, P.P., Ramaiah, D.: DNA-assisted long-lived excimer formation in a cyclophane. Angew. Chem. Int. Ed. **47**(44), 8407–8411 (2008). doi:10.1002/anie.200803162
6. Neelakandan, P.P., Sanju, K.S., Ramaiah, D.: Effect of bridging units on photophysical and DNA binding properties of a few cyclophanes. Photochem. Photobiol. **86**(2), 282–289 (2010). doi:10.1111/j.1751-1097.2009.00660.x
7. Bouas-Laurent, H., Castellan, A., Daney, M., Desvergne, J.P., Guinand, G., Marsau, P., Riffaud, M.H.: Cation-directed photochemistry of an anthraceno-crown ether. J. Am. Chem. Soc. **108**(2), 315–317 (1986). doi:10.1021/ja00262a032
8. Inoue, M.B., Medrano, F., Inoue, M., Raitsimring, A., Fernando, Q.: A new chelating cyclophane and its complexation with Ni2+, Cu2+, and Zn2+: spectroscopic properties and allosterism via ring contraction. Inorg. Chem. **36**(11), 2335–2340 (1997). doi:10.1021/ic9614374
9. Inoue, M.B., Velazquez, E.F., Medrano, F., Ochoa, K.L., Galvez, J.C., Inoue, M., Fernando, Q.: Binuclear copper(II) chelates of amide-based cyclophanes. Inorg. Chem. **37**(16), 4070–4075 (1998). doi:10.1021/ic980238c

10. Inoue, M.B., Muñoz, I.C., Machi, L., Inoue, M., Fernando, Q.: Structural and spectroscopic studies of binuclear Cu2+ and Co2+ complexes with an amide-based naphthalenophane. Inorg. Chim. Acta. **311**(1–2), 50–56 (2000). doi:10.1016/S0020-1693(00)00305-4
11. Inoue, M.B., Muñoz, I.C., Inoue, M., Fernando, Q.: X-ray structures and fluorescence spectra of binuclear Zn2+ and Cd2+ complexes of an amide-based naphthalenophane. Inorg. Chim. Acta. **300–302**, 206–211 (2000). doi:10.1016/s0020-1693(99)00565-4 doi
12. Soberanes, Y., Arvízu-Santamaría, A.G., Machi, L., Navarro, R.E., Inoue, M.: Fluorescent aza-cyclophanes derived from diethylenetriaminepentaacetic acid (DTPA), and their complexation with Gd(III). Polyhedron. **35**(1), 130–136 (2012). doi:10.1016/j.poly.2012.01.007
13. Pina, J., de Melo, J.S., Pina, F., Lodeiro, C., Lima, J.C., Parola, A.J., Soriano, C., Clares, M.P., Albelda, M.T., Aucejo, R., García-España, E.: Spectroscopy and coordination chemistry of a new bisnaphthalene–bisphenanthroline ligand displaying a sensing ability for metal cations. Inorg. Chem. **44**(21), 7449–7458 (2005). doi:10.1021/ic050733q
14. Neelakandan, P.P., Nandajan, P.C., Subymol, B., Ramaiah, D.: Study of cavity size and nature of bridging units on recognition of nucleotides by cyclophanes. Org. Biomol. Chem. **9**(4), 1021–1029 (2011). doi:10.1039/C0OB00673D
15. Dhaenens, M., Lehn, J.-M., Vigneron, J.-P.: Molecular recognition of nucleosides, nucleotides and anionic planar substrates by a water-soluble bis-intercaland-type receptor molecule. J. Chem. Soc. Perkin Trans. 2 **0**(7), 1379–1381 (1993). doi:10.1039/P29930001379
16. Abe, H., Mawatari, Y., Teraoka, H., Fujimoto, K., Inouye, M.: Synthesis and molecular recognition of pyrenophanes with polycationic or amphiphilic functionalities: artificial plate-shaped cavitant incorporating arenes and nucleotides in water. J. Org. Chem. **69**(2), 495–504 (2004). doi:10.1021/jo035188u
17. Covington, A.K., Paabo, M., Robinson, R.A., Bates, R.G.: Use of the glass electrode in deuterium oxide and the relation between the standardized pD (paD) scale and the operational pH in heavy water. Anal. Chem. **40**(4), 700–706 (1968). doi:10.1021/ac60260a013
18. Pitarch, J., Clares, M.P., Belda, R., Costa, R.D., Navarro, P., Orti, E., Soriano, C., Garcia-Espana, E.: Zn(II)-coordination and fluorescence studies of a new polyazamacrocycle incorporating 1H-pyrazole and naphthalene units. Dalton Trans. **39**(33), 7741–7746 (2010). doi:10.1039/C0DT00204F
19. Alarcón, J., Albelda, M.T., Belda, R., Clares, M.P., Delgado-Pinar, E., Frías, J.C., García-España, E., González, J., Soriano, C.: Synthesis and coordination properties of an azamacrocyclic Zn(II) chemosensor containing pendent methylnaphthyl groups. Dalton Trans. (2008). doi:10.1039/b808993k
20. Albelda, M., Díaz, P., García-España, E., Bernardo, M., Pina, F., Melo, J., Soriano, C., Luis, S.: Polyamines containing naphthyl groups as pH-regulated molecular machines driven by light. Chem. Commun. (2001). doi:10.1039/B104311K
21. Machi, L., Santacruz, H., Sánchez, M., Inoue, M.: Cd^{2+}-sensiting bichromophore: excimer emission from an EDTA-methylnaphthalene derivative. Inorg. Chem. Commun. **10**(5), 547–550 (2007). doi:10.1016/j.inoche.2007.01.015 doi
22. Machi, L., Santacruz, H., Sánchez, M., Inoue, M.: Bichromophoric naphthalene derivatives of ethylenediaminetetraacetate: fluorescence from intramolecular excimer, protonation and complexation with Zn^{2+} and Cd^{2+}. Supramol. Chem. **18**(7), 561–569 (2006)
23. Albelda, M.T., García-España, E., Gil, L., Lima, J.C., Lodeiro, C., de Melo, J.S., Melo, M.J., Parola, A.J., Pina, F., Soriano, C.: Intramolecular excimer formation in a tripodal polyamine receptor containing three naphthalene fluorophores. J. Phys. Chem. B. **107**(27), 6573–6578 (2003). doi:10.1021/jp0343032
24. Clares, M.P., Aguilar, J., Aucejo, R., Lodeiro, C., Albelda, M.T., Pina, F., Lima, J.C., Parola, A.J., Pina, J., de Melo, J.S., Soriano, C., García-España, E.: Synthesis and H+, Cu2+, and Zn2+ coordination behavior of a bis(fluorophoric) bibrachial lariat aza-crown. Inorg. Chem. **43**(19), 6114–6122 (2004). doi:10.1021/ic049694t
25. de Melo, J.S., Pina, J., Pina, F., Lodeiro, C., Parola, A.J., Lima, J.C., Albelda, M.T., Clares, M.P., Garcia-España, E., Soriano, C.: Energetics and dynamics of naphthalene polyaminic derivatives. Influence of structural design in the balance static vs dynamic excimer formation. J. Phys. Chem. A. **107**(51), 11307–11318 (2003). doi:10.1021/jp036149p
26. Kawakami, J., Komai, Y., Sumori, T., Fukushi, A., Shimozaki, K., Ito, S.: Intramolecular excimer formation and complexing behavior of 1,n-bis(naphthalenecarboxy)oxaalkanes as fluorescent chemosensors for calcium and barium ions. J. Photochem. Photobiol. A. **139**(1), 71–78 (2001). doi:10.1016/S1010-6030(00)00421-4
27. Aucejo, R., Alarcón, J., García-España, E., Llinares, J.M., Marchin, K.L., Soriano, C., Lodeiro, C., Bernardo, M.A., Pina, F., Pina, J., de Melo, J.S.: A new ZnII tweezer pyridine-naphthalene system—an Off–On–Off system working in a biological pH window. Eur. J. Inorg. Chem. **2005**(21), 4301–4308 (2005). doi:10.1002/ejic.200500403
28. Machi, L., Muñoz, I.C., Pérez-González, R., Sánchez, M., Inoue, M.: Pyrene bichromophores composed of polyaminopolycarboxylate interlink: pH response of excimer emission. Supramol. Chem. **21**(8), 665–673 (2009)
29. Pérez-González, R., Machi, L., Inoue, M., Sánchez, M., Medrano, F.: Fluorescence and conformation in water-soluble bis(pyrenyl amide) receptors derived from polyaminopolycarboxylic acids. J. Photochem. Photobiol. A. **219**(1), 90–100 (2011). doi:10.1016/j.jphotochem.2011.01.022
30. de Melo, J.S., Albelda, M.T., Diaz, P., Garcia-Espana, E., Lodeiro, C., Alves, S., Lima, J.C., Pina, F., Soriano, C.: Ground and excited state properties of polyamine chains bearing two terminal naphthalene units. J. Chem. Soc. Perkin Trans. **2**(5), 991–998 (2002). doi:10.1039/B110769K
31. Pina, F., Lima, J.C., Lodeiro, C., de Melo, J.S., Díaz, P., Albelda, M.T., García-España, E.: Long range electron transfer quenching in polyamine chains bearing a terminal naphthalene unit. J. Phys. Chem. A. **106**(35), 8207–8212 (2002). doi:10.1021/jp025848j
32. Sudmeier, J.L., Reilley, C.N.: Nuclear magnetic resonance studies of protonation of polyamine and aminocarboxylate compounds in aqueous solution. Anal. Chem. **36**(9), 1698–1706 (1964). doi:10.1021/ac60215a006
33. Bates, R.G.: Standardization of acidity measurements extension of the pH concept to mixed solvents and heavy water. Anal. Chem. **40**(6), 28A–38A (1968). doi:10.1021/ac60262a723
34. Reijenga, J., van Hoof, A., van Loon, A., Teunissen, B.: Development of methods for the determination of pKa values. Anal. Chem. Insights **8**, 53–71 (2013). doi:10.4137/ACI.S12304
35. Jones, R.L., Wilson, W.D.: Effect of ionic strength on the pKa of ligands bound to DNA. Biopolymers. **20**(1), 141–154 (1981). doi:10.1002/bip.1981.360200110
36. Inoue, M.B., Santacruz, H., Inoue, M., Fernando, Q.: Binuclear Gd3+ complex of a 34-membered macrocycle with six carboxymethyl arms: X-ray structures, formation constants, NMR, EPR, and 1H NMR relaxivities. Inorg. Chem. **38**(7), 1596–1602 (1999). doi:10.1021/ic981015p
37. Inoue, M.B., Oram, P., Inoue, M., Fernando, Q.: 1H NMR and protonation constants of new metal-chelating macrocycles, oxocyclopolyamines with pendant carboxymethyl groups, and the stabilities of their Mg2+ and Ca2+ complexes. Inorg. Chim. Acta. **232**(1–2), 91–98 (1995). doi:10.1016/0020-1693(94)04389-d doi
38. Dean, J.A., Lange, N.A.: Lange's Handbook of Chemistry. McGraw-Hill, New York (1985)